Nanoscale

Field enhancement of MoS2: visualization of enhancement and effect of the number of layers

Journal:	*Nanoscale*
Manuscript ID	NR-ART-07-2018-005650.R1
Article Type:	Paper
Date Submitted by the Author:	13-Sep-2018
Complete List of Authors:	Sakamoto, Masanori; Hiroshima University Saitow, Ken-ichi; Hiroshima University, Natural science center for Basic R&D

Journal Name

ARTICLE

Field enhancement of MoS_2: visualization of enhancement and effect of the number of layers

Received 00th January 20xx,
Accepted 00th January 20xx

DOI: 10.1039/x0xx00000x

www.rsc.org/

Masanori Sakamoto[a] and Ken-ichi Saitow*[a,b]

Two-dimensional transition metal dichalcogenides (2D TMDCs) are layered semiconductor materials with unique electronic and optical properties. In the family of 2D TMDCs, molybdenum disulphide (MoS_2) is a promising material for next-generation optoelectorical devices due to its high mobility and characteristic properties. The properties of 2D TMDCs, as well as device performances, can be further improved by a field enhancement effect. However, field enhancement has not been reported to date in the 2D TMDCs family. Here, we show the field enhancement of MoS_2 and its dependence on the number of layers (5–850 layers). Measurements of the fluorescence intensity of a dye solution, crystal violet, were used to visualize the enhancement factor (EF) for a MoS_2 flake as a map. The EFs on the map were independently confirmed by *x-y-z* size measurements of the same MoS_2 flake with an atomic force microscope. Furthermore, the obtained *x-y-z* sizes of a MoS_2 flake were used for the finite-difference time-domain (FDTD) calculations to evaluate field enhancement. As a result, a MoS_2 flake with a specific thickness (ca. 80 layers) gave the highest enhancement with EF=100. Theoretical calculations based on Mie scattering theory also confirmed the experimental EF mapping results, the dependence on the number of layers, and the component analysis of field enhancement. As another crucial point, large and small enhancement effects were attributed to electric field and charge transfer effects, respectively, both of which depend on the number of layers. A transition region of these effects was indicated at around 300-400 layers.

1. Introduction

Optical excitation of a noble metal nanostructure can generate localized surface plasmons, which results in a large electric field as "plasmon resonance".[1,2] When molecules located near the surface are excited by this localized electric field, their Raman and/or fluorescence intensities are enhanced. This phenomenon has been recognized as surface-enhanced Raman scattering (SERS),[3, 4] surface-enhanced fluorescence (SEF),[1,2,5] or metal-enhanced fluorescence. According to recent reviews on SEF, typical materials for SEF are gold (Au) or silver (Ag), and their typical enhancement factors (EFs) are 10–100,[5] except for several high values, such as EF = 1340 for bow-tie-shaped Au nanoantenna[6] and EF = 4000 for Au–Ag bimetallic nanopetals.[7] Thus, EFs for SEF are much lower than the typical EFs for SERS, i.e., EF = 10^5–10^6.[8] Such a reduced EF for SEF is due to the electronic structure of metals with a high density of states, which causes fluorescence quenching via energy transfer from excited molecules to the metal.

Semiconductors have recently attracted much attention as field-enhancement materials due to their low cost and large enhancement effect. The large enhancement is due to "Mie resonance",[9-14] which occurs in dielectric materials such as semiconductors. Semiconductors have several specific properties, such as a high refractive index, no electronic states in the band gap, and direct or indirect optical transitions. In particular, an indirect band gap can reduce fluorescence quenching due to the lack of electronic states in the band gap and the forbidden electronic relaxation. For example, Hayashi et al. reported an EF of 140 for gallium phosphide (GaP).[15] Wells et al. reported an EF of 120 for silicon (Si) nanopillar structures.[16] In our previous study, the SEF of Si particles was investigated and a particle size of 500 nm gave the maximum EF of 180.[17a,b] As our recent study, it was found that TiO_2 porous layer gives extraordinary field enhancement as EF=500.[17d]

Two-dimensional transition metal dichalcogenides (2D TMDCs) are promising semiconductor materials with unique electronic and optical properties. Among the 2D TMDCs, molybdenum disulphide (MoS_2) is one of the most popular materials because 1) its bandgap energy can be tuned according to the number of layers, 2) the optical transition changes from an indirect type to a direct type by being scaled down to monolayers,[18] 3) it has high mobility in a field-effect transistor (>200 cm^2 V^{-1} s^{-1}),[19] 4) it has flexibility and durability (high Young's modulus of 238-270 GPa, cf. stainless steel at 205 GPa),[20] 5) and it has low toxicity (high cell viability ≥80%).[21] These excellent properties of MoS_2 provide a material for

[a] Department of Chemistry, Graduate School of Science, Hiroshima University, 1-3-1 Kagamiyama, Higashi-hiroshima, Hiroshima 739-8526, Japan
[b] Natural Science Center for Basic Research and Development (N-BARD), Hiroshima University, 1-3-1 Kagamiyama, Higashi-hiroshima, Hiroshima 739-8526, Japan
Electronic Supplementary Information (ESI) available: [details of any supplementary information available should be included here]. See DOI: 10.1039/x0xx00000x

photocatalysts for hydrogen evolution reaction,[22] phototransistors,[23] optical biosensors,[24] solar cells,[25] and their flexible and/or wearable devices in near future. The efficiencies of these devices can be increased with an enhancement material such as MoS_2, which provides a large field enhancement of incident and/or radiated light. However, there have been no reports on field enhancement due to 2D TMDCs. For instance, SERS of MoS_2 has been reported for a monolayer or a few atomic layers, but its mechanism is attributed to a charge transfer effect.[26-29] In addition, it has not been understood so far whether or not the field enhancement effect of 2D TMDCs occurs. As another aspect, there have been no reports on SEF for all the family of 2D TMDCs.

Here, we demonstrate the field enhancement of MoS_2 flakes by measurement of fluorescence spectra for a dye molecule in a solution. The enhancement effect was evaluated as a function of the number of MoS_2 layers (5-850 layers) and was visualized by enhancement mapping of fluorescence at the same positions observed using atomic force microscopy (AFM). The experimental results are compared with those from calculations using the same sample and the same region and discussed with respect to two different enhancement mechanisms, which depend on the layer thickness.

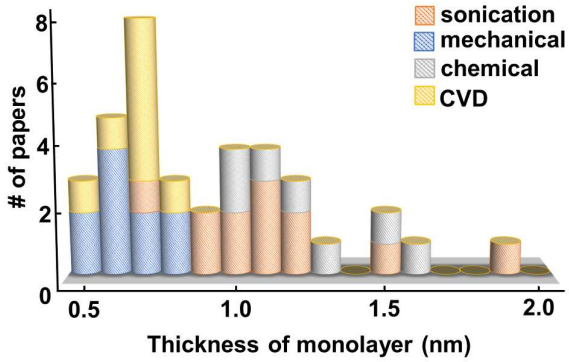

Fig. 1 Thickness distribution of MoS_2 monolayer. These thicknesses are reported in recent papers, listed in Table S1. All the thickness is evaluated by measuring AFM and depend on preparation methods of the monolayer. The methods are in the following; sonication: exfoliation by sonication in a solvent; mechanical: exfoliation by the scotch tape; chemical: exfoliation by a lithium intercalation method, e. g. butyllithium; CVD: synthesis from a chemical vapor deposition method.

2. Experimental section

2.1 Preparation of MoS_2 flakes and enhanced substrate using drop-casting.

MoS_2 flakes were produced by a liquid-phase-exfoliation method using sonication.[30] Commercial MoS_2 powder (Kojundo kagaku. Co) was dispersed in a binary solvent (2-propanol: water =7:3 (v/v)) at a concentration of 30 mg/ml without further purification. The solution dispersed with MoS_2 was prepared by bath sonication (Yamato 3510, Bronson) for 5 h, followed by centrifugation at 6500 rpm for 60 min (5430, Eppendorf). After centrifugation, the top two-thirds of the dispersion solution was gently extracted by pipetting. The enhanced substrate was prepared by drop-casting the dispersion solution of MoS_2 onto a silicon (Si) wafer (p-type, (100) face) was cleaned with piranha solution and dried for 5 h at room temperature. The MoS_2 flakes on the Si wafer were then washed three times with methanol. The thickness of the MoS_2 flakes was measured using AFM (SPM-9700, Shimadzu) or with a laser microscope (OLS4000, Olympus). The number of layers was determined by dividing the thickness measured with AFM by a monolayer thickness as 1.2 nm, which is used in the present study. There are two reasons for choosing 1.2 nm. Firstly, 1.2 nm is the average thickness of monolayer MoS_2 prepared by a sonication method (Fig.1, Table S1). Secondly, our sonication procedures are the same to the previous study, giving the monolayer thickness of 1.2 nm.[30]

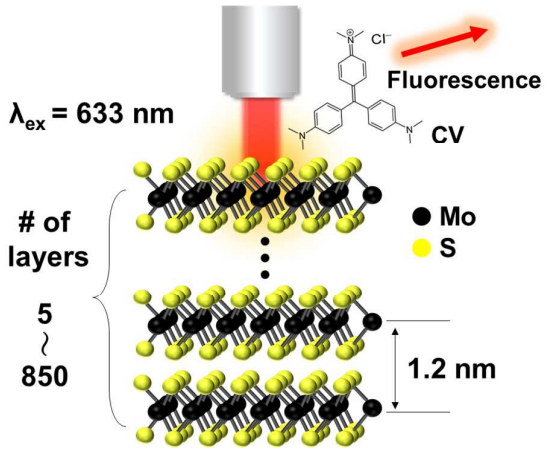

Fig. 2 Schematic diagram of field enhancement of MoS_2 evaluated from surface enhanced fluorescence of crystal violet (CV). The value of 1.2 nm is the average thickness of MoS_2 monolayer, prepared by a liquid-exfoliation method with sonication, based on the data of Fig. 1 and Table S1.

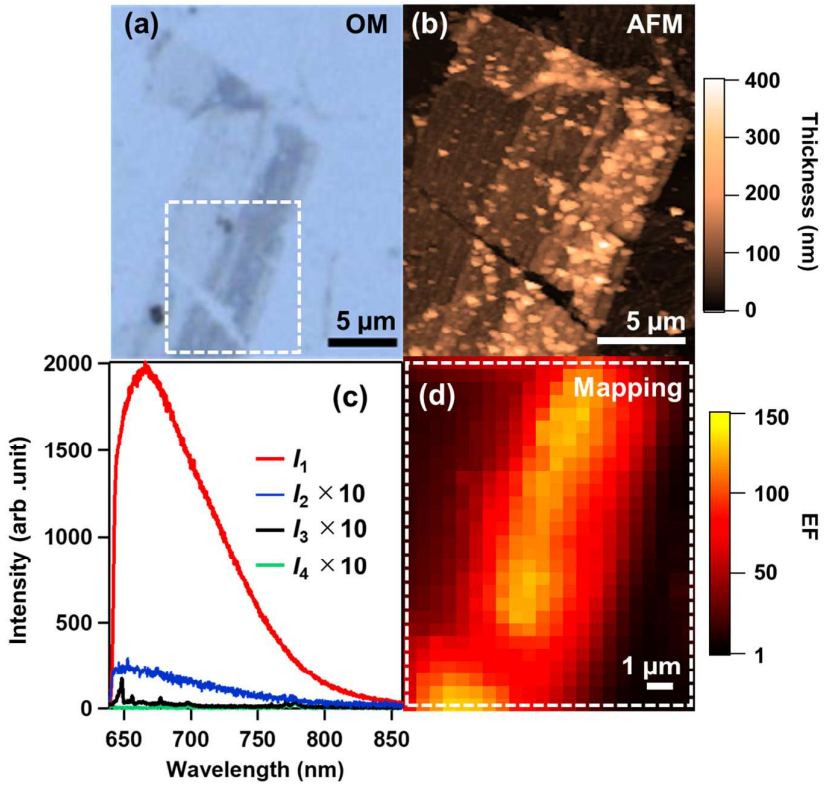

Fig. 3 (a) Optical microscopy (OM) and (b) atomic force microscopy (AFM) images of MoS_2 flakes on a silicon wafer formed by drop-casting. (c) Fluorescence spectra of the crystal violet (CV) solution. The red curve, I_1, shows the CV spectrum in the presence of a MoS_2 flake with a thickness of ca. 100 nm (ca. 80 layers). The blue curve, I_2, shows the CV spectrum in the absence of the MoS_2 flake. The black curve, I_3, shows a background spectrum of I_1 with methanol as the solvent and with the MoS_2 flakes. The green curve, I_4, shows a background spectrum of I_2 with methanol as the solvent and without the MoS_2 flakes. The EF of the fluorescence intensity is obtained using these four spectra, according to $EF=(I_1-I_3)/(I_2-I_4)$. Since the intensities of I_2 , I_3, I_4 in comparison to I_1 are too small to be evaluated, the data of I_2 , I_3, and I_4 are multiplied by 10 for the clarity in the figure. (d) EF mapping for fluorescence of CV at the peak wavelength in the white square area shown in Fig. 3a.

2.2 Enhancement spectra measurements and estimation of EF

Fluorescence spectra of the crystal violet (CV) as a dye solution were measured with a confocal microscope spectrometer (HR800, Horiba Jobin Yvon) at an excitation wavelength of 632.8 nm using a He-Ne laser, as displayed in Fig. 2. The molecular structure of CV is also shown in Fig. 2. The laser power was attenuated to ca. 70 μW in front of an optical cell involving samples. As samples, MoS_2 flakes attached onto the Si wafer was immersed in a CV solution of the cell. An objective lens (SMLPLN, 100×, Olympus) with a long working distance was used to measure the spectrum of the sample solution under a cover glass of the cell. The optical cell for measurement of the spectrum was designed to provide a solution layer between the cover glass and the MoS_2 flakes and has been described elsewhere.[17a-d] The dye solution used was CV dissolved in methanol to a concentration of 3.6×10^{-5} M. The EF of fluorescence intensity was obtained from the measurement of four spectra: (1) the intensity of the

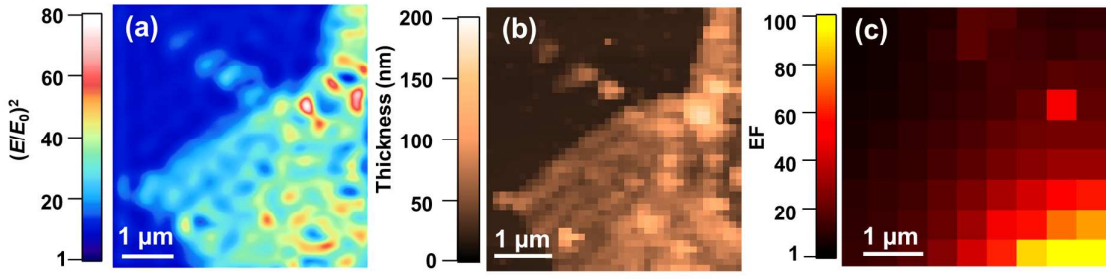

Fig. 4 (a) EF mapping of electric field (E: Electric field intensity with MoS_2, E_0: without MoS_2) obtained from FDTD calculation for the surface measured using AFM shown in Fig. 4b. (c) EF mapping of the fluorescence of CV at the same surface shown in Fig. 4a and 4b. As for the grid sizes, Figs.4a, b, and c are set to 10 nm (FDTD), 100 nm (AFM), and 500 nm (fluorescence micro spectroscopy), respectively.

fluorescence spectrum of the CV solution with the MoS_2 flakes (I_1), (2) the intensity of the fluorescence spectrum of the CV solution without the MoS_2 flakes (I_2), (3) the intensity of the background spectrum of (1) with methanol as the solvent and with the MoS_2 flakes (I_3), and (4) the intensity of the background spectrum of (2) with methanol as the solvent and without the MoS_2 flakes (I_4). The EF of the fluorescence intensity was then obtained using these four spectra, according to $EF=(I_1-I_3)/(I_2-I_4)$.[17a-d,31] These EFs were evaluated as an average with the standard deviation.[32]

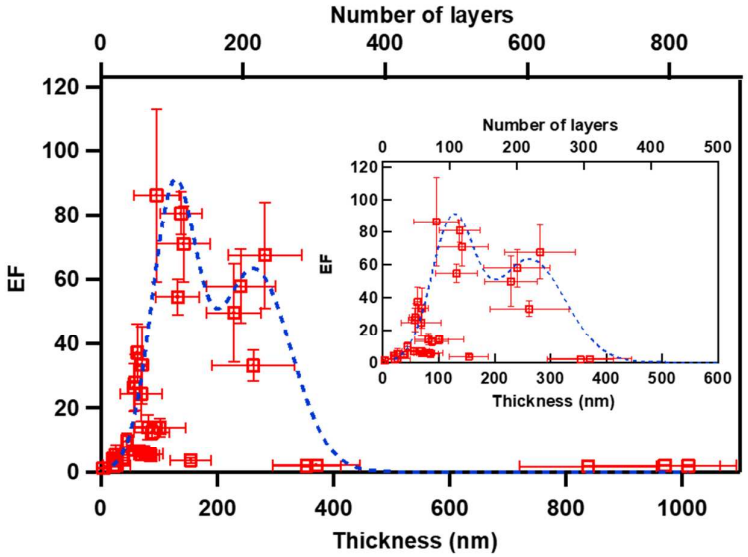

Fig. 5 EF of fluorescence for CV with MoS_2 flake as a function of the number of layers (thickness). The inset figure shows the EF for MoS_2 with thicknesses of 5–600 nm. Blue dashed curves are fitting curves of two Gaussian functions for guide to eye.

2.3 Evaluation and calculation of the MoS_2 flakes.

The finite-difference time-domain (FDTD) and the extinction efficiency (Q_{ext}) calculations based on the Mie scattering theory were performed for the same sample, the same region, and the same conditions as the experimental data. The height data obtained by AFM were used as the thickness of MoS_2 layer for the FDTD calculation, i.e., the computer-aided- was obtained by importing AFM data directly into the FDTD software. The electric field distribution on the surface of the MoS_2 flakes was calculated using the FDTD method with the FullWAVE commercial software (Cybernet Systems Co., Ltd.). Q_{ext} was calculated using the Mieplot software (ver. 4.05.02, Philip Laven) and the software developed by NASA.[33] For these calculations, the refractive index of MoS_2 reported by Rubio-Bollinger et al.[34] at an excitation wavelength of 632.8 nm was used, in addition to n = 1.33 as the refractive index for the surrounding medium (methanol).

3. Results and discussion

Fig. 3a and 3b show typical images of MoS_2 flakes on a Si wafer captured using optical microscopy (OM) and AFM, respectively. The colour bar shows the height of the MoS_2 flakes, which corresponds to the thickness. The MoS_2 flakes are several micrometers in the *x*- and *y*- directions and 10–450 nm in the *z*- direction (thickness). Fig. 3c shows typical fluorescence spectra of CV as a dye solution, with (red) and without (blue) a MoS_2 flake with a thickness of ca. 100 nm (ca. 80 layers) as well as background signals (black and green). The fluorescence intensity increases in the presence of MoS_2 and its EF was estimated to be 100. In addition, the enhancement effect is visualized by mapping EFs of fluorescence intensity at 650 nm, as shown in Fig. 3d. This is the first time that SEF have been observed experimentally and by EF mapping for 2D TMDCs.

Fig. 4a shows EF mapping of the electric field obtained by FDTD calculation, which was conducted using the *x*-*y*-*z* position measured from an AFM image, as shown Fig. 4b (see Fig. S1). The calculation result reveals the electric field enhancement in the presence of MoS_2, and the result is in good agreement

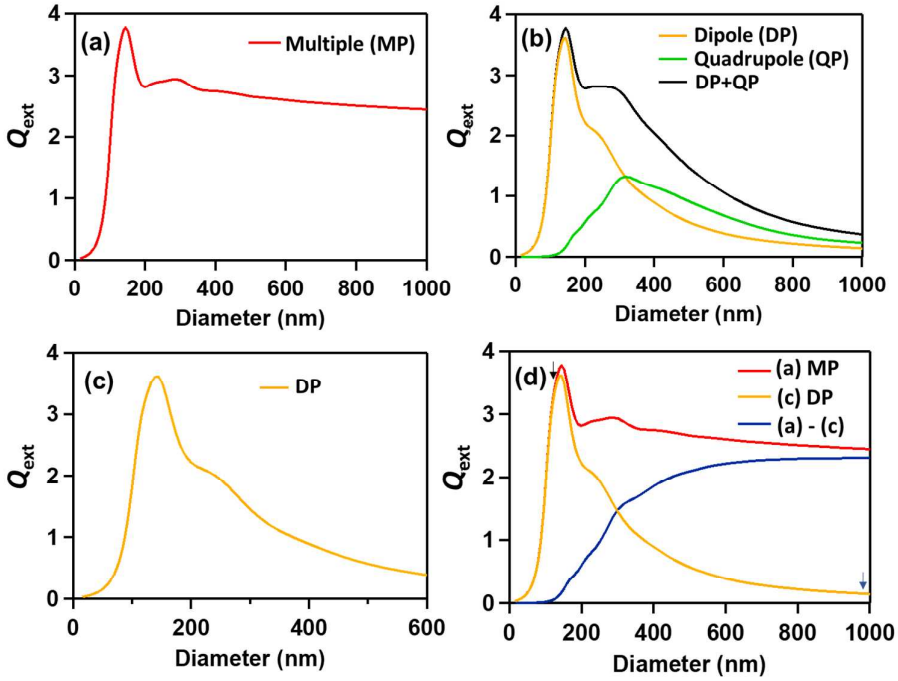

Fig. 6 Extinction efficiency (Q_{ext}) as a function of the diameter of a spherical particle of MoS_2 calculated with (a) multiple component as a linear combination of electric and magnetic dipole, quadrupole, and higher-order modes, (b) electric and magnetic dipole (DP) and quadrupole (QP) modes, and (c) electric and magnetic dipole (DP) mode. (d) The blue curve is the Q_{ext} obtained from the subtraction of the dipole (DP) from the multiple component. For the comparison, the multiple and the dipole components are represented by red and yellow curves, respectively, both of which are the same to the ones in Fig. 6a and 6c.

with the EF mapping of fluorescence with CV shown in Fig. 4c, which is measured using the same MoS_2 flake. Therefore, the electric field enhancement of MoS_2 was confirmed from the experimental data and calculations at the same position of the same MoS_2 flake. Similar results are also demonstrated in the other MoS_2 flakes, as shown in Fig.S2. As for the grid sizes, Figs.4a, b, and c are set to 10 nm, 100 nm, and 500 nm, respectively.[35]

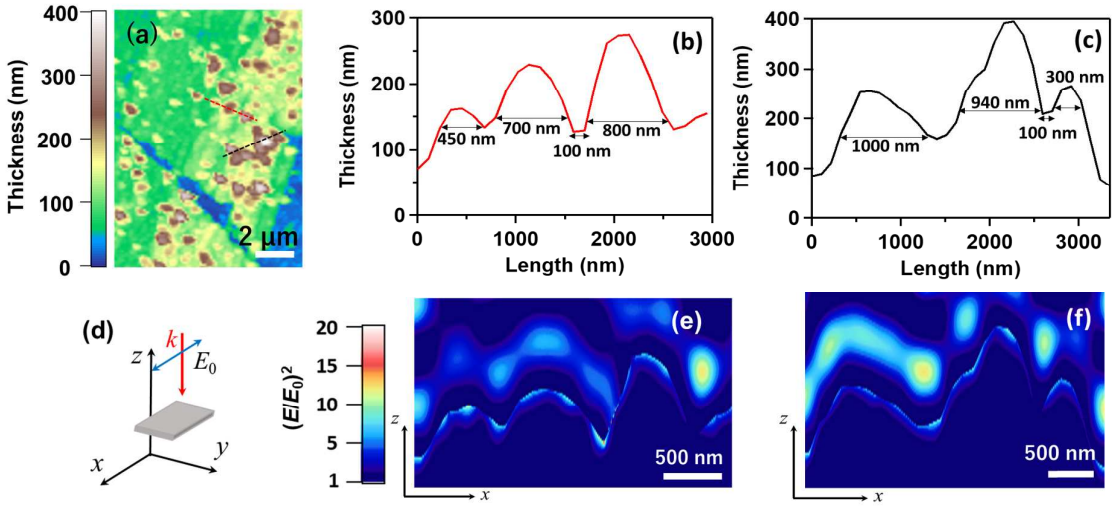

Fig. 7 (a) AFM image of MoS_2 flakes. The data is the same to Fig.3b, but the thickness is expressed by full colors. The line profiles of AFM image (a) are shown in (b) and (c), corresponding to red and black dashed lines, respectively. (d) Schematic diagram of the optical configuration between light and MoS_2 layer for the FDTD calculation. Linearly polarized light is irradiated from the upper side to the MoS_2 along *z*-direction upon the excitation wavelength of 632.8 nm. The red arrow, blue arrow, and grey plain represent the direction of incident light, and its polarization direction, and MoS_2 layer, respectively. FDTD calculations of (b) and (c) demonstrate EF mappings of electric fields (e) and (f), respectively. In these calculations, the MoS_2 layer is set to be immersed in methanol, which is the same to the experimental condition.

Fig. 5 shows the experimental data for the EF as a function of the MoS_2 thickness. The upper axis shows the number of layers of MoS_2 estimated from the thickness, i.e. the thickness of monolayer=1.2 nm. All error bars of EF and thickness (number of layers) denote σ, where the σ is a standard deviation from an average.[32] MoS_2 flakes with a thickness of 100 nm (ca. 80 layers) have the highest EF, and those with over 400 nm had the smallest EFs (*vide infra*). To understand the dependence on the layered MoS_2 thickness, the extinction efficiency (Q_{ext}) was calculated at an excitation wavelength of 632.8 nm, based on Mie scattering theory.[9-14] Fig. 6 shows Q_{ext} for MoS_2 as a function of the diameter of the MoS_2 flakes, immersed in methanol. Note that the profile of EF as a function of the number of layers in Fig. 5 is in good agreement with that of Q_{ext} as a function of the diameter in Fig. 6. Thus, a large electric field is ensured to be produced using MoS_2 flakes with a size in the range of 100-300 nm. In other word, it was

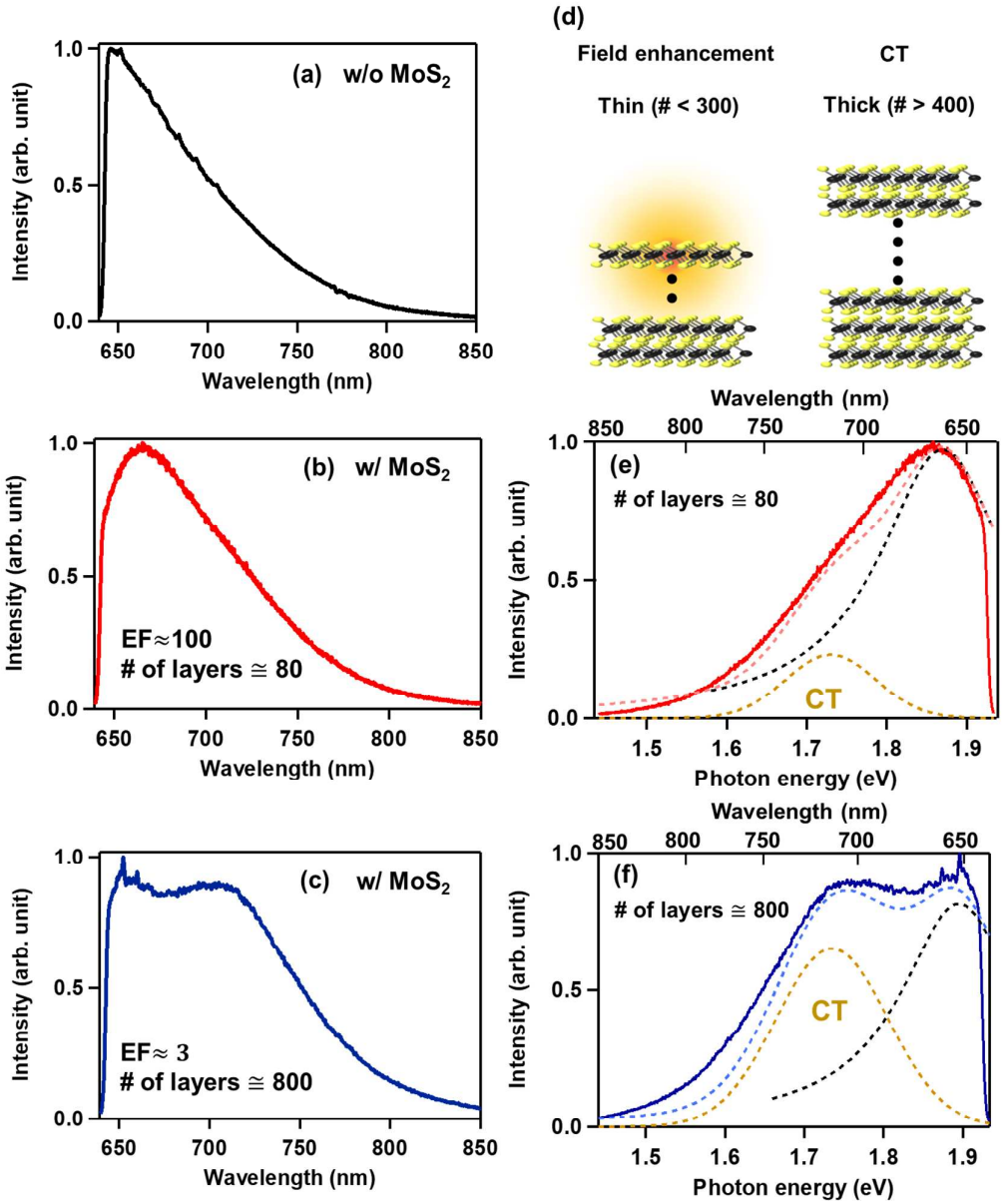

Fig. 8 Fluorescence spectra of CV solution (a) without MoS_2, (b) with ca. 80 MoS_2 layers, and (c) with ca. 800 MoS_2 layers. (d) Schematic diagram of thin and thick MoS_2 layers. A thin MoS_2 flake, the number of layers, #, < 300, gives an enhanced fluorescence by field enhancement effect, whereas a thick MoS_2 flake, # > 400, gives an enhanced fluorescence by a charge transfer effect. Fluorescence spectra of (b) and (c) are analyzed by decomposing into a charge transfer (CT) band and a nonCT band using two Gaussian functions. The data of (e) and (f) represent analyzed spectra of (b) and (c), respectively. Yellow and black dashed curves represent CT and nonCT bands, respectively.

found that the preparation of MoS_2 flakes with 100-300 nm thickness gives larger EF.

Next, we discuss a mechanism of higher EF, based on the results of Figs. 5 and 6. According to these data, it is revealed that the EF profile of Fig. 6 is in good agreement with the Q_{ext} calculated using terms of the electric and magnetic dipoles,[33] as shown in 6c, whereas it deviates from the Q_{ext}, as shown in Fig. 6a, calculated from the linear combination of multiple components,[33] i.e. electric and magnetic dipoles, quadrupoles, and higher-order components. Thus, both these agreement and deviation indicate that a principle component of large EF is not higher-order components but a lower-order component such as the dipoles. Since this is the first time what a component involved in the Q_{ext} is a critical factor to produce larger EF of 2D material, the finding in the present study is a promising result to design and/or characterize field enhancement of 2D materials. A further theoretical research on field enhancement of a 2D material, on the other hand, will

be important, because experimental results in Fig. 5 were investigated by the thickness as a size of MoS_2, whereas the Q_{ext}, based on Mie resonance in Fig. 6, was calculated using the diameter of a spherical particle as a size of MoS_2. As another important mechanism, we evaluated whether or not nanogaps, steps, and edges on the MoS_2 surface could give larger EF. Here, we show line profiles of AFM image and conducted FDTD calculations of the line profiles, as displayed in Fig. 7. As a result, the EFs are high as EF=10-15 at around nanogaps, steps, and edges. However, these values even though the maximum are 8 times smaller than those of the thickness effect of EF=100, as shown in Fig. 5. Consequently, it was concluded that larger EFs are not given by surface structures such as nanogaps, steps, and edges but by the thickness of MoS_2 with 100-300 nm. Such the thickness of MoS_2 governs significant field enhancement, whose mechanism is due to the electric and magnetic dipoles.

Here, we discuss the shape of CV fluorescence spectra measured with and without MoS_2. Figs. 8a, b, and c show fluorescence spectra for CV solutions without MoS_2, with MoS_2 (ca. 80 layers), and with MoS_2 (ca. 800 layers), respectively. The profiles for the former two are similar, whereas that for the latter is significantly different. Similar features were observed in the other thicknesses (Figs. S5, 6). Namely, the fluorescence spectrum for CV with thicker MoS_2 has a shoulder at around 700-800 nm, which is considered to be a charge transfer (CT) band, based on the following three reasons. First, the luminescence wavelength via CT between CV and MoS_2 after the excitation can be estimated as 1.73 eV, i.e., the energy difference between the conduction band of MoS_2 and the highest occupied molecular orbital (HOMO) of CV (see Fig. S3). This energy corresponds to a wavelength of around 720 nm, which is almost equal to the shoulder in Fig. 8c. Second, the luminescence intensity of MoS_2 is so weak that it cannot give the shoulder in Fig. 8c, because the intensity of MoS_2 itself is 6 times smaller than that of CV (Fig. S4). In addition, the MoS_2 spectral peak is located at 650 nm (Fig. S4), which is different from the wavelength of the shoulder around 700-800 nm (Fig. 8c). Third, according to several reports on SERS by MoS_2, the EF is very small as EF=10-100[26,29,31] by comparing with a typical SERS as EF = 10^5–10^6 using a metal.[8] The mechanism of their small EFs have been attributed to CT between MoS_2 and a molecule.,[26-29] i.e. the charge transfer from MoS_2 to a molecule is attributed to cause the enhancement of Raman intensity. A small enhancement effect due such the CT may be involved in the present system. Therefore, it was concluded that the large and small enhancements are due to electric field and CT effects, respectively, depending on the thickness of MoS_2 (Fig. 8d). A transition region due to either the field enhancement or charge transfer effects was considered to be at around the number of layers of MoS_2 = 300-400; larger EFs for thin MoS_2 (the number of layers, #, < 300) and small EFs for thick MoS_2 (# > 400) (*vide supra)*.

Finally, we describe the reason why the MoS_2 with 800 layers, as shown in Fig. 8c, gives significant CT band. This is because the electronic band structure of MoS_2 with 800 layers is almost same to that of 80 layers, i.e. band structures of MoS_2 with # > 4 are nearly equal to that of the bulk MoS_2.[36-38] Under these situations, there are two factors for describing the mechanism. Firstly, we quantified the spectral component by decomposing CV fluorescence spectra into nonCT and CT bands using two Gaussian functions, as shown in Figs. 8e and 8f. These results indicate that ratios of "CT/nonCT" for MoS_2 with 80 and 800 layers become 1.0/10.3 and 1.0/1.7, respectively. Namely, the spectral component of CT band increases as the layer thickness of MoS_2 increases. Secondly, Fig. 5 showed that a thicker MoS_2 gives very small enhancement (ca. # > 400). Namely, the EF of 80 layers was 30 times higher than that of 800 layers. As for the calculated result, the Q_{ext} at the 100 nm (80 layers) is also 25 times greater than that of 1000 nm (800 layers). Therefore, it was recognized that the CT band of MoS_2 (# < 300) is hidden by the strong field enhancement effect of MoS_2, although the energy bands of MoS_2 flakes is similar to one other.

4. Conclusion

In summary, the field enhancement effect of MoS_2 flakes (5-850 layers) was investigated according to the fluorescence intensity of a dye solution and by visualization with EF mapping. The results obtained for the EF effect were examined by calculation using the same MoS_2 flake at the same position. MoS_2 flakes with a thickness of ca. 100 nm (ca. 80 layers) gave a large EF of 100 for fluorescence. These results were in good agreement with those from the extinction efficiency Q_{ext} and FDTD calculations. The large and small enhancement effects were attributed to electric field and charge transfer, respectively, both of which are dependent on the layer thickness. Namely, the former and latter effects were established by MoS_2 flakes with the number of layers < 300 and > 400, respectively. A principle component giving a significant field enhancement was the electric and magnetic dipole of MoS_2 involved in the Q_{ext}. It is promised that the current results for the field enhancement of MoS_2 will lead to an improved understanding of electric field enhancement in the 2D TMDC family and to higher performance devices with 2D TMDCs.

Conflicts of interest

There are no conflicts to declare.

Acknowledgements

We acknowledge reviewers for giving valuable comments as well as critical readings of manuscript. We thank for Mr. Akagi, Mr. Tanabe, and Mr. Sekiguchi of Cybernet systems Co., Ltd. for special assistances for FDTD calculations. K.S. acknowledges the Funding Program for the Next Generation World-Leading Researchers (GR073) of the Japan Society for the Promotion of Science (JSPS), a Grant-in-Aid for Scientific Research (A) (15H02001) from JSPS, and the "Structure Control

and Function" of PRESTO/Japan Science and Technology Agency (JST).

Notes and references

1 J. Park, J. Kim, and J.M Nam, Chemical science, 2017, **8**, 4696-4704.
2 M. Li, S. K. Cushing, and N. Wu , *Analyst*, 2015, ***140***, 386-406.
3 S. Y. Ding, E.M.You, Z. Q .Tian, and M. Moskovits, *Chem Soc Rev*, 2017, ***46***, 4042-4076.
4 S. Schlücker, *Angewandte Chemie International Edition* 2014, ***53***, 4756-4795.
5 M. Bauch, K. Toma, M. Toma, Q. Zhang, and J. Dostalek, *Plasmonics*, 2014, ***9***, 781-799.
6 A. Kinkhabwala, Z. Yu, S. Fan, Y. Avlasevich, K. Müllen, and W. Moerner, *Nature Photonics*, 2009, **3**, 654–657.
7 C.-C. Fu, G. Ossato, M. Long, M. Digman, A. Gopinathan, L. Lee, E. Gratton, and M. Khine, *Applied Physics Letters*, 2010, **97**, 203101.
8 K. Willets, V.RP, *Annual Review of Physical Chemistry*, 2007, ***58***, 267-297.
9 Y. Tanaka, G. Obara, A. Zenidaka, N. N. Nedyalkov, M. Terakawa, and M. Obara, *Opt Express.*, 2010, **18**, 27226.
10 V. Rutckaia, F. Heyroth, A. Novikov, M. Shaleev, M. Petrov, and J. Schilling, *Nano Lett.*, 2017, **17**, 6886-6892
11 A. Kuznetsov, A. Miroshnichenko, M. Brongersma, Y. Kivshar, and B. Luk'yanchuk, *Science*, 2016, **354**, aag2472.
12 J. Cambiasso, G. Grinblat, Y. Li, A. Rakovich, E. Cortés, and S. A. Maier, *Nano Lett.*, 2017, **17**, 1219–1225.
13 P. Albella, R. Osa, F. Moreno, and S. Maier, *Acs Photonics*, 2014, **1**, 524–529.
14 P. Albella, A. Poyli, M. Schmidt, S. Maier, F. Moreno, J. Sáenz, and J. Aizpurua, *J.Phys.Chem .C.*, 2013, **117**, 13573–13584.
15 S. Hayashi, Y. Takeuchi, S. Hayashi, and M. Fujii, *Chemical Physics Letters*, 2009, **480**, 100–104.
16 S. M. Wells, I. A. Merkulov, I. I. Kravchenko, N. V. Lavrik, and M. J. Sepaniak, *ACS Nano*, 2012, **6**, 2948–59.
17 (a) K. Saitow, H. Suemori, and H. Tamamitsu, *Chem. Commun.*, 2014, **50**, 1137–40. (b) H. Sun, S. Miyazaki, H. Tamamitsu, and K. Saitow, *Chem. Commun.*, 2013, **49**, 10302-10304. (c) H. Tamamitsu and K.Saitow, *Chem. Phys. Lett.*, 2014, **591**, 37-42. (d) K. Yoshihara, M. Sakamoto, H. Tamamitsu, M. Arakawa, and K. Saitow, *Adv. Opt. Mater.*, 2018, DOI:10.1002/adom.201800462.
18 Q. H. Wang, K.K-Zadeh, A. Kis, J. N. Coleman, and M.S. Strano, *Nat Nanotechnol.*, 2012, ***7***, 699-712.
19 Radisavljevic, Radenovic, Brivio, Giacometti, and Kis, *Nature Nanotechnology*, 2011, **6**, 147–150.
20 S. Bertolazzi, J. Brivio, and A. KIs, *ACS Nano*, 2011, ***5***, 9703-9709.
21 E. Chng and M. Pumera, *RSC Advances*, 2015, **5**, 3074-3080
22 A. Laursen, S. Kegnaes, S. Dahl, I. Chorkendorff, *Energy Environ. Sci.*, 2012, **5**, 5577-5591
23 J. Lin, H. Li, H. Zhang, and W. Chen, *Applied Physics Letters*, 2013, **102**, 203109
24 S. Barua, H. Dutta, S. Gogoi, R. Devi, and R. Khan, *ACS Applied Nano Materials*, 2018, **1**, 2–25.
25 M. Tsai, S. Su, J. Chang, D. Tsai, C. Chen, C. Wu, L. Li, L. Chen and J. He, *ACS Nano*, 2014, ***8***, 8317-8322.
26 Y. Yin, P. Miao, Y. Zhang, J. Han, X. Zhang, Y. Gong, L. Gu, C. Xu, T. Yao, P. Xu, Y. Wang, B. Song, and S. Jin, *Advanced Functional Materials*, 2017, **27**, 1606694
27 Y. Y. Xu, C. Yang, S. Z. Jiang, B. Y. Man, M. Liu, C. S. Chen, C. Zhang, Z. C. Sun, H. W. Qiu, H. S. Li, D. J. Feng, and J. X. Zhang, *Appl Surf Sci.*, 2015, **357**, 1708–1713.
28 X. Ling, W. Fang, Y. Lee, P. Araujo, X. Zhang, J. Nieva, Y. Lin, J. Zhang, J. Kong, and M. Dresselhaus, *Nano Lett.*, 2014, **14**, 3033–3040.
29 C. Muehlethaler, C. Considine, V. Menon, W.-C. Lin, Y.-H. Lee, and J. Lombardi, *Acs Photonics*, 2016, **3**, 1164–1169.
30 J. Shen, Y. He, J. Wu, C. Gao, K. Keyshar, X. Zhang, Y. Yang, M. Ye, R. Vajtai, J. Lou, and P. Ajayan, *Nano Lett.*, **15**, 5449–5454.
31 The EFs, 10-100, are estimated from the ratio of intensities with and without MoS_2 in refs. 26 and 29, the method of which is the same as the current system. For the case of ref. 29, the large EFs, mentioned as 10^5-10^6, are estimated from a different method, i.e. EF per a molecule.
32 As for the data in the y axis, each EF value was obtained as an average of 30-50 spectra for the I_1 and 5 spectra for the I_2, I_3 and I_4. For the data in the *x*-axis, each thickness was obtained as an average height in the region of 2 μmx2 μm, which corresponds to the irradiation area of laser light to MoS_2. Thus, the error bars in x- and y- axes denote their standard deviations σ.
33 (a)https://www.giss.nasa.gov/staff/mmishchenko/brf/; (b)Bohren, C. F. Huffman, D. R. Absorption and Scattering of Light by Small Particles; Wiley-VCH: Weinheim, 2004. (c) K. Saitow, T. Yamamura, and T. Minami, *J Phys Chem C.*, 2008, **112**, 18340–18349
34 G. Rubio-Bollinger, R. Guerrero, D. Lara, J. Quereda, L. Vaquero-Garzon, N. Agraït, R. Bratschitsch, and A. Castellanos-Gomez, *Electronics*, 2015, **4**, 847–856.
35 The special resolution of Fig. 4c. is due to a far field measurement, owing to the diffraction limit of light.
36 A. Splendiani, L. Sun, Y. Zhang, T. Li, J. Kim, and C.-Y. Chim, G. Galli, and F. Wang, Nano Lett, 2010, **10**, 1271-1275
37 S. Ahmad, S. Mukherjee, *Graphene*, 2014, **3**, 52-59
38 R. Ganatra and Q. Zhang, *ACS Nano*, 2014, **8**, 4074–99.

Graphical abstract

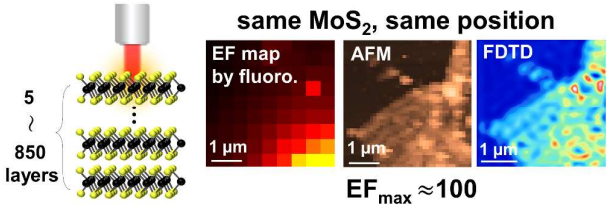

Field enhancement is investigated by spectroscopy, microscopes, and calculations at the same position. Enhancement factor and mechanism change by thickness.